



Polypropylene/Waste Ground Rubber Tire Powder Foams: A Study of the Relationship Between Processing and Structure Using Supercritical Carbon Dioxide

Zhen Xiu Zhang,¹ Shu Ling Zhang,^{1,2} Zhen Xiang Xin,^{1,3} Jin Kuk Kim^{1*}

¹School of Nano and Advanced Materials Engineering, Gyeongsang National University, Gyeongnam, Jinju, 660-701, South Korea. Tel: (+82) (0)55-751-5299. Fax: (+82) (0)55-753-6311. Email: rubber@gsnu.ac.kr.

²Alan G. MacDiarmid Lab, College of Chemistry, Jilin University, Changchun, 130012, People's Republic of China

³Key Laboratory of Rubber-plastics of Ministry of Education, Qingdao University of Science and Technology, Qingdao, 266042, People's Republic of China.

(Received: 12 September, 2007; published: 15 November, 2007)

Abstract: In this study, processing-structure relationships in polypropylene (PP)/waste ground rubber tire powder (WGRT) foams made using supercritical carbon dioxide as a physical blowing agent were investigated. In order to investigate the relationship between structure and properties of PP/WGRT foams, it was necessary to make samples with a wide range of controlled structures. For this reason, a systematic investigation of the relationship between processing conditions and structure was performed based on a statistical experimental design. Regression analysis was conducted on the data and expressions were developed to quantify the relationships between structural parameters and processing conditions. The samples were saturated with carbon dioxide at high temperature and high pressure and the saturated specimens were expanded during the pressure-quench process. The importance of the individual processing parameters was determined. Statistical analysis of data showed that saturation temperature was the most important factor determining cell size, cell density and relative density. By controlling the foaming conditions, PP/WGRT samples having the same foam density and different cell size or having the same cell size and different foam density were produced.

Keywords: foam; polypropylene; waste ground rubber tire powder; microstructure; supercritical carbon dioxide

Introduction

In the last century polymer foams have been an important category of industrial plastics. Polymer foams can be used in many fields, such as insulation, packaging, structures, and filters [1-3]. Some remarkable properties have been noted for microcellular foams. Specifically, they can offer good mechanical properties and a reduction on material costs and weight at the same time [4].

Various blowing agents are used to produce polymer foams. The selection of the blowing agent mainly depends on the basic material and foaming process. The blowing agents may be divided into two major groups, physical and chemical. The physical blowing agents are usually compressed gases and volatile liquids such as nitrogen, carbon dioxide, hydrocarbons, ketones, and alcohols. Chemical blowing agents are generally solid organic or inorganic materials, which evolve gas by a

chemical reaction or decomposition within a temperature range. In many applications, the use of a physical blowing agent is appropriate. A pressure-quench method described by Goel and Beckman is widely used for making microcellular polymers via supercritical carbon dioxide (scCO₂) [5]. They found that the microcellular structure could be achieved by rapid depressurization to allow the cells nucleation and growth as in the batch process after saturating polymers with scCO₂.

Our lab is researching the development of thermoplastic vulcanizates from waste ground rubber tires [6]. The present work is continuation of our research efforts to obtain 'value added products' from PP/WGRT blends and deals with the production of microcellular composites from the same by scCO₂. In order to investigate the relationship between structure and properties of PP/WGRT foams, it was necessary to make samples with a wide range of controlled structures. For this reason, a systematic investigation was performed based on a statistical experimental design. Various processing conditions were used and the structures of the resulting foams were examined using a scanning electron microscope (SEM). Regression analysis was conducted on the data and expressions were developed to quantify the relationship between structural parameters and processing conditions. Moreover, the importance of the individual processing parameters was determined using a statistical analysis of data.

Results and Discussion

In order to make samples with a wide range of controlled structures, the effects of processing parameters on the structure of polypropylene/waste ground rubber tire powder (PP/WGRT) foams was explored in the work. After preparing the samples using conditions given in Table I, the expanded samples were fractured in liquid N₂ and their internal structures were examined using SEM. A summary of the experimental results on structure is also given in Table I.

The dependence of cell size, cell density, and relative density on the foaming conditions is shown in Fig 1– 3. In this section, using these plots, the effects of saturation temperature, saturation pressure and WGRT content on the foam structure were discussed. The statistical analysis were performed in two steps. First, all model terms were considered and statistical parameters were calculated. In the second step, only significant terms (terms with confidence levels of greater than 95%) were considered. The regression expressions for cell size (D), cell density (N_0), and relative density (ρ_r) are presented in eqs. (1), (2), and (3), respectively.

$$\ln(D) = 132.434 - 1.761P - 1.594T - 0.006426f + 0.0123PT + 0.004732T^2 \quad (1)$$

$$N_0 = -1.543 \times 10^{12} + 1.004 \times 10^{10}P + 1.996 \times 10^{10}T - 5.855 \times 10^8 f - 4.95 \times 10^7 PT + 9.305 \times 10^6 Pf + 2.562 \times 10^6 Tf - 1.212 \times 10^8 P^2 - 6.411 \times 10^7 T^2 \quad (2)$$

$$\rho_r = -25.737 + 0.427P + 0.323T - 0.0341f - 0.002988PT + 0.0002419Tf - 0.0009574T^2 \quad (3)$$

The effects of foaming conditions on the cell size are given in Fig 1. Obviously, the cell size increases when saturation temperature and saturation pressure increase or WGRT powder content decreases. Statistical analysis of data indicates that saturation temperature has the greatest effect on the cell size. The effect of saturation pressure is less than that of saturation temperature, and the effect of WGRT powder is not significant.

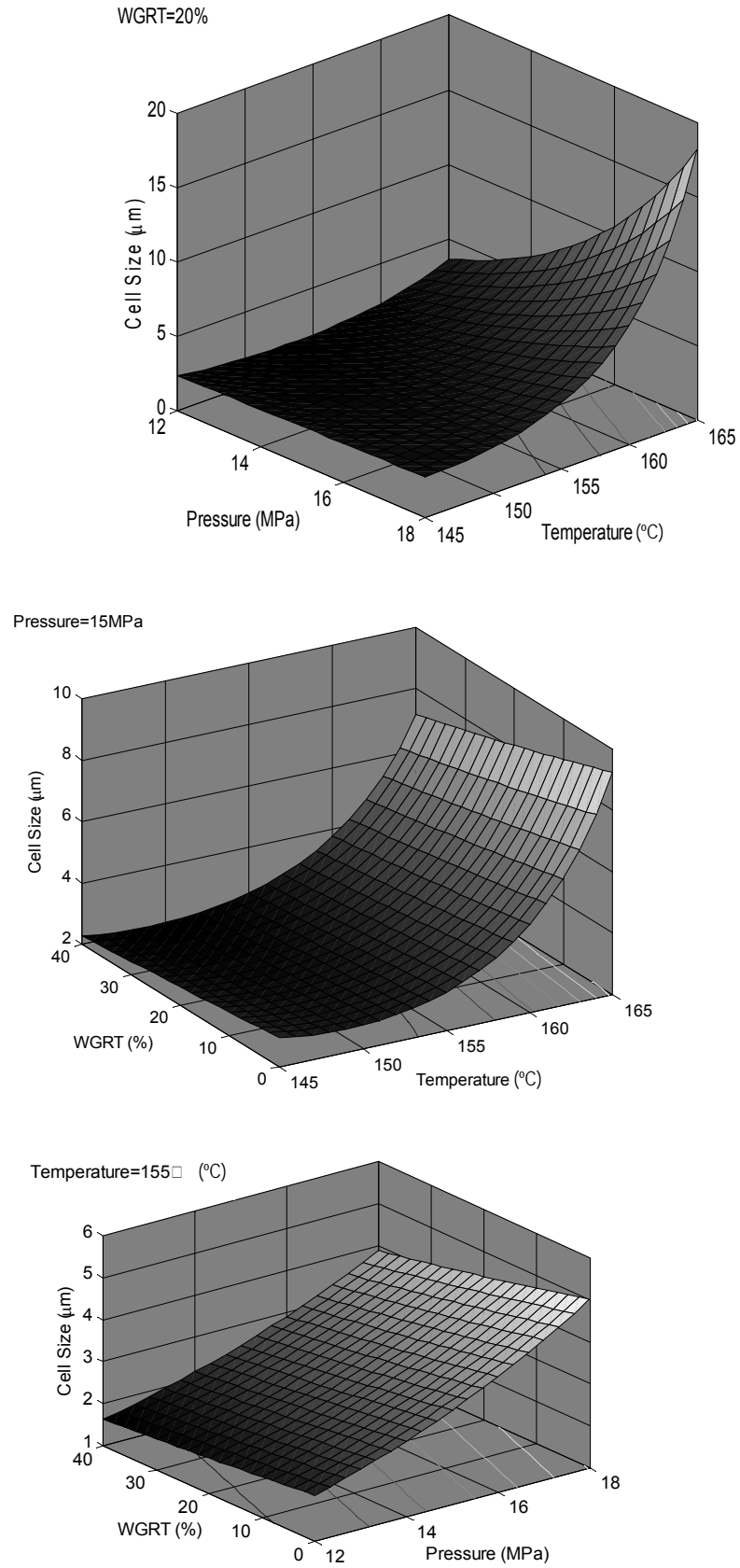


Fig. 1. Effect of foaming conditions on the cell size of PP/WGRT foams. The surfaces represent the fitted regression model (eq. 1).

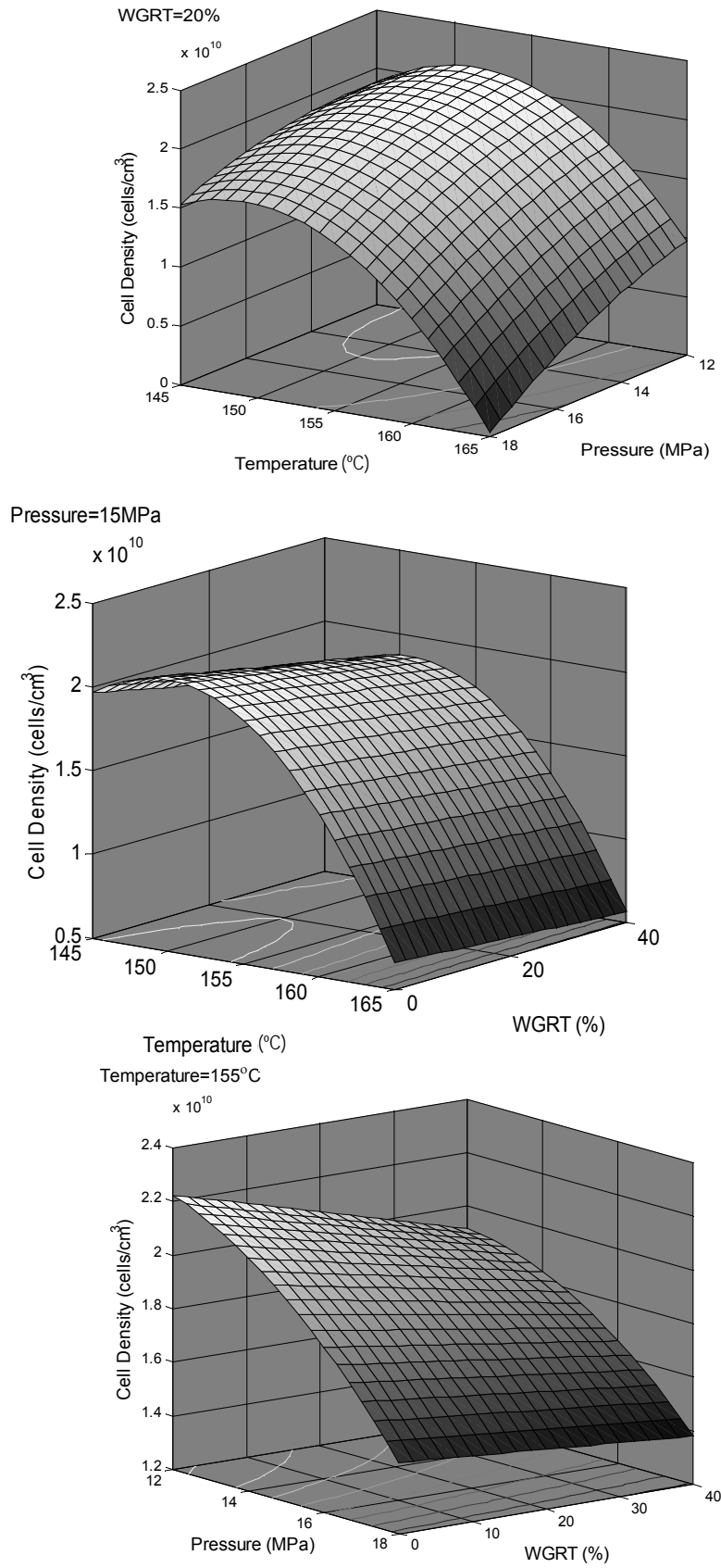


Fig. 2. Effect of foaming conditions on the cell density of PP/WGRT foams. The surfaces represent the fitted regression model (eq. 2).

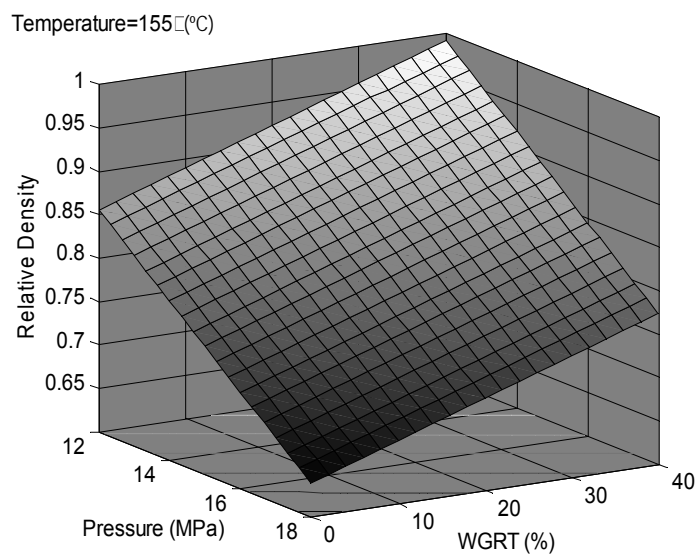
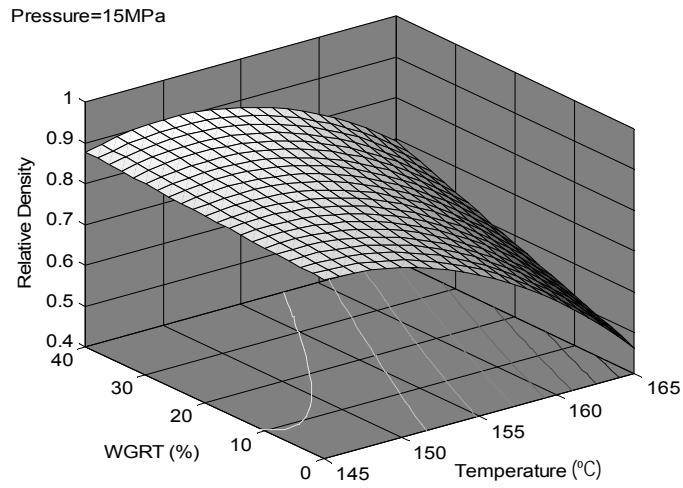
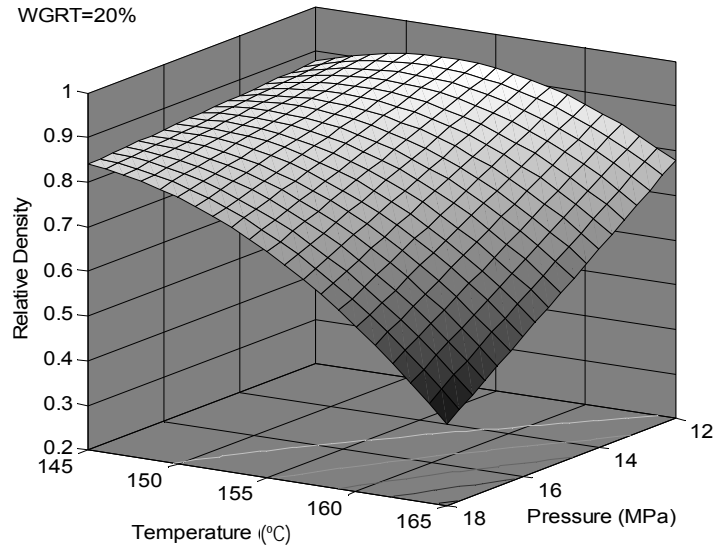


Fig. 3. Effect of foaming conditions on the relative density of PP/WGRT foams. The surfaces represent the fitted regression model (eq. 3).

The effects of foaming conditions on the cell density are given in Fig 2. Obviously, the cell density decreases with the increase of saturation pressure, whereas the cell density slightly increases then decreases with the increase of saturation temperature. It is noticeable that the cell density decreases with the increase of WGRT content at lower saturation temperature or saturation pressure, whereas the cell density slightly increases at higher saturation pressure and saturation temperature. Statistical analysis of data exhibits that saturation temperature is the most important factor determining the cell density. The importance of saturation pressure is less than that of saturation temperature. WGRT content has the smallest effect on the cell density.

The effects of foaming conditions on the relative density are given in Fig 3. Obviously, the relative density increases when saturation temperature and saturation pressure decrease or WGRT powder content increases. Statistical analysis of data shows that saturation temperature is the most important factor determining relative density, followed by saturation pressure and WGRT content. Moreover, there is obvious interaction between saturation temperature and saturation pressure. The conclusion is obtained due to the evaluation of probability. If the value of probability is less than 0.05, model term is significant. The value of probability is less than 0.0001 for PT, so PT term is significant, namely the interaction between saturation temperature and saturation pressure is obvious.

Effect of saturation temperature

Scanning electron micrographs of PP/WGRT (60/40) specimen foams produced at two different temperatures are shown in Fig 4. In the experiment the saturation pressure and saturation time were kept at 12 MPa and 3 h respectively and the saturation temperature increased from 145 to 165 °C. The cell density first slightly increases then decreases as the saturation temperature increases from 145 to 165 °C, while the average cell size always increases. The cells are discrete and almost spheres at lower temperature, surrounded by thick walls (Fig. 4a). As saturation temperature increases, the expansion increases and the cell walls become thinner (Fig. 4b).

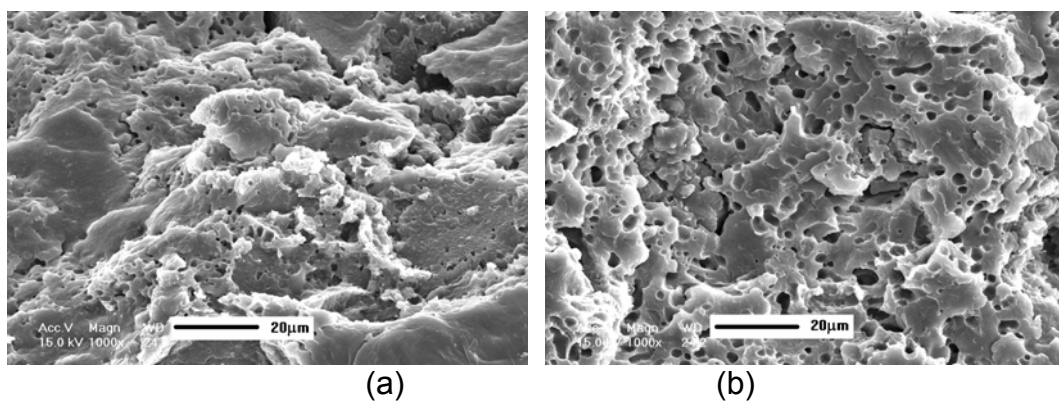


Fig. 4. SEM micrographs of PP/WGRT (60/40) specimen produced at different saturation temperature (a) 145 °C and (b) 165 °C. P = 12MPa and t = 3 h.

When the saturation temperature increases, the crystalline phase can be partly or totally disrupted. Thus CO₂ is expected to be dissolved in and diffuse through both the amorphous phase and the disrupted part of the crystalline phase. Therefore both the deformability and foamability of PP/WGRT (60/40) specimen are improved. Thus

conditions become more favorable for PP/WGRT (60/40) specimen to foam and for the cells to grow bigger in size. The reason for a maximum in cell densities is that both cell nucleation and cell growth rates increase with saturation temperature and both phenomena compete for the gas available in the system. This leads to a trade-off at some optimum temperature where a maximum in cell densities is observed. The decrease of the relative densities is ascribed to cell size increase and the cell walls becoming thinner.

Effect of saturation pressure

Scanning electron micrographs of PP/WGRT (80/20) foams produced at low and high levels of saturation pressure are shown in Fig 6. In the experiment the saturation temperature and saturation time were kept at 155 °C and 3 h respectively and the saturation pressure increased from 12 to 18 MPa. The cell density decreases as the saturation pressure increases from 12 to 18 MPa, while the average cell size increases. The resulting foams are closed cell, since the cells are discrete and not connected. When the saturation pressure is very low, the extent of the CO₂ induced-melting temperature depression is low, namely the amount of CO₂ dissolved in PP/WGRT (80/20) specimen is low. Thus PP/WGRT (80/20) is stiff and its deformability and foamability are small.

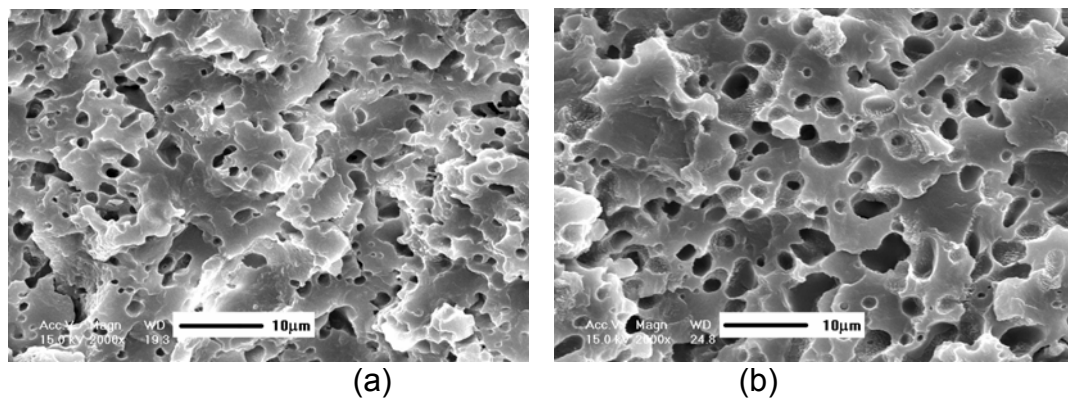


Fig. 5. SEM micrographs of PP/WGRT (80/20) specimen produced at different saturation pressure (a) 12 MPa and (b) 18 MPa. T = 155 °C and t = 3 h.

When it is very high, both the CO₂ induced-melting temperature depression and the amount of CO₂ dissolved in PP/WGRT (80/20) specimen become very important. As a result, the melt strength of PP/WGRT (80/20) specimen becomes weak, namely its deformability and foamability are large. Thus increasing saturation pressure becomes more favorable for PP/WGRT (80/20) specimen to foam and for the cells to grow bigger in size and the corresponding cell density and relative density decrease. It is noticeable that the cell size and the relative density are more sensitive to the saturation pressure (the plot has a large slope) at higher saturation temperature (see Fig 1 and Fig 3).

Effect of WGRT content

Scanning electron micrographs of PP/WGRT foams produced at two different compositions are shown in Fig 6. In the experiment the saturation pressure, saturation temperature and saturation time were kept at 18 MPa, 165 °C and 3 h respectively. The cell density decreases at the lower saturation temperature or

saturation pressure as the WGRT content increases from 0 to 40 wt %, while the cell density slightly increases at the higher saturation temperature and saturation pressure. The cell size decreases as the WGRT content increases, whereas the relative density increases. It is known that the foamability of polymers is affected by the sorption of gas in the polymer and the mechanisms of cell nucleation and cell growth are influenced by the amount of the gas dissolved in polymer and the rate of gas diffusion [7, 8]. Increasing the WGRT powder content increases the viscosity of PP/WGRT blends [9] and provides more channel through which CO₂ can quickly escape from the composites [10, 11], which limits cell nucleation and growth. Therefore the cell density and cell size decrease.

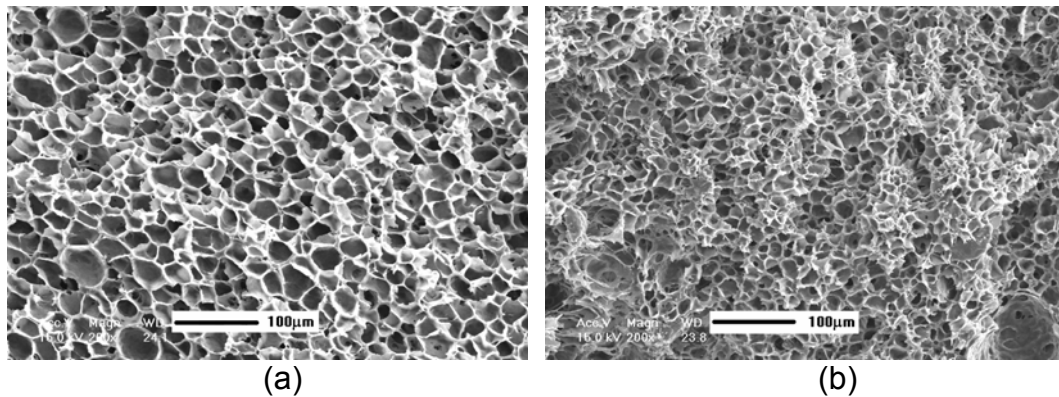


Fig. 6. SEM micrographs of PP/WGRT specimen produced at different WGRT content (a) 0 wt% and (b) 40 wt%. P = 18MPa, T = 165 °C and t = 3 h.

However, the heterogeneous nucleation of WGRT is not negligible at the higher saturation temperature and saturation pressure. Namely higher saturation temperature and saturation pressure can supply enough CO₂ dissolved in samples so that the effect of heterogeneous nucleation of WGRT becomes obvious, thus the cell density slightly increases. In addition, since WGRT powder cannot be foamed, increasing the amount of WGRT powder in the sample will increase the relative density.

Relationship between cell size and foam density

The goal of this study is to control microstructure of PP/WGRT foams by controlling the process parameters. The plot of cell size versus foam density (Fig. 7) indicates that by controlling the foaming conditions, foams having the same foam density and different cell sizes or having the same cell size and different cell density can be produced. For example, PP/WGRT (100/0) foam produced at 12 MPa, 165 °C and PP/WGRT (80/20) foam produced at 15 MPa, 165 °C exhibit the same foam density of 0.584 g/cm³, but have different cell sizes of 4.26 and 6.05 μm. PP/WGRT (100/0) foam produced at 15 MPa, 155 °C and PP/WGRT (60/40) foam produced at 12 MPa, 165 °C exhibit the same cell size of 3.12 μm, but have different foam density of 0.655 and 0.830 g/cm³. In order to conduct a systematic investigation of the effect of cell size and foam density on the properties of the expanded polymer, it is very important to produce foam specimens with controlled foam density and cell size in this way.

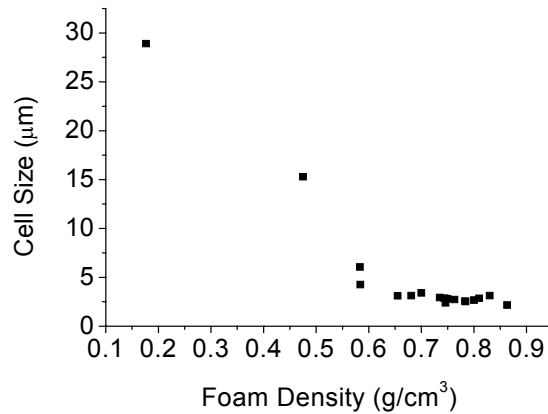


Fig. 7. Correlation between cell size and foam density for specimens produced under different conditions.

Conclusions

The effects of foaming conditions on the structure of polypropylene/waste ground rubber tire powder (PP/WGRT) foams were investigated. By controlling the foaming conditions, including saturation temperature, saturation pressure and WGRT content, a wide range of foam densities and cell sizes could be produced. The results of the statistical analysis show that saturation temperature is the most important factor determining cell size, cell density and relative density. It was observed that by controlling the foaming conditions, PP/WGRT samples having the same foam density and different cell size or having the same cell size and different foam density could be produced. These variations in cell size and foam density could be used and be tailor-made for certain applications.

Experimental part

Materials and sample preparation

Polypropylene (Co-PP, B391M) was manufactured by SK Corporation. The waste ground rubber tire powder was produced by wet grinding method and its particle size was characterized to be 30-40 μm by SEM (Fig. 8).

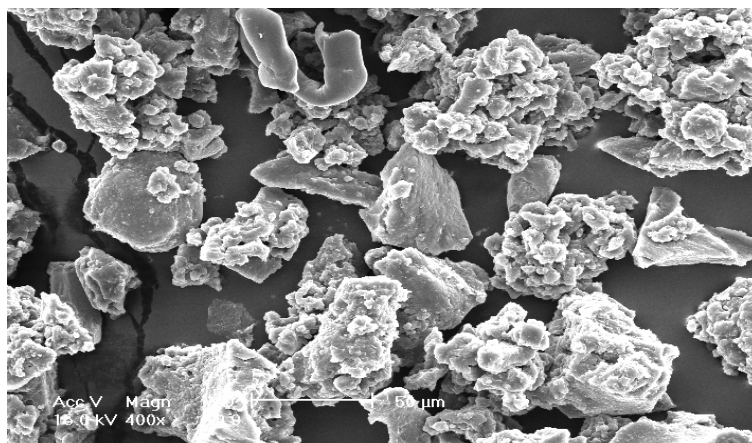


Fig. 8. SEM micrograph of 30-40 μm waste ground rubber tire powder.

CO₂ with a purity of 99.95% was supplied by Hyundai Gas Inc. Blends were prepared with an internal mixer and their composition is given in Table 1. The mixing conditions were 180 °C, 60 rpm, and 10 min. After mixing, the plate samples of the blends with 3.0 mm thickness were compression-molded at 180 °C for 6 min.

Foam preparation

The foams were prepared with a pressure-quench method described by Goel and Beckman [5]. Plate samples (20 × 4 × 3 mm) were enclosed in high-pressure vessel. The vessel was flushed with low-pressure CO₂ for about 3 min and pressurized to the saturated vapor pressure CO₂ at room temperature with CO₂ withdrawn from a liquid CO₂ cylinder and preheated to desired temperature. Afterward, the pressure was increased to the desired pressure by a high-pressure pump and maintained at that pressure for 3 h. After saturation, the pressure was quenched to atmospheric pressure within 3 s and the samples were taken out. Then foam structure was allowed to full growth during rapid depressurization. The processing condition is listed in Table 1.

Tab. 1. Processing conditions and foam characteristics for samples.

Temperature (°C)	Pressure (MPa)	WGRT (Wt %)	Cell size D (μm)	Cell density N ₀ (cells/cm ³)	Relative density
145	12	0	2.38	2.09×10 ¹⁰	0.871
145	12	40	2.16	1.68×10 ¹⁰	0.918
145	15	20	2.56	1.87×10 ¹⁰	0.859
145	18	0	3.12	1.62×10 ¹⁰	0.795
145	18	40	2.86	1.39×10 ¹⁰	0.854
155	12	20	2.51	1.97×10 ¹⁰	0.860
155	15	0	3.11	1.96×10 ¹⁰	0.765
155	15	20	2.93	1.82×10 ¹⁰	0.806
155	15	20	2.80	1.87×10 ¹⁰	0.823
155	15	20	2.72	1.84×10 ¹⁰	0.837
155	15	20	2.85	1.85×10 ¹⁰	0.816
155	15	20	2.84	1.86×10 ¹⁰	0.817
155	15	40	2.67	1.85×10 ¹⁰	0.844
155	15	20	2.84	1.86×10 ¹⁰	0.817
165	12	0	4.26	1.15×10 ¹⁰	0.682
165	12	40	3.12	8.96×10 ⁹	0.875
165	15	20	6.05	4.86×10 ⁹	0.640
165	18	0	28.90	3.16×10 ⁸	0.200
165	18	40	15.28	5.35×10 ⁸	0.500

Foam characterization

The foamed samples were fractured in liquid nitrogen, coated with an approximately 10-nm thick layer of gold on the fractured surface, and observed with a Philips XL 30S scanning electron microscope (SEM). The cell diameter (*D*) is the average of all the cells on the SEM photo, usually more than 100 cells were measured.

$$D = d / (\pi / 4) \quad (4)$$

where d is the measured average diameter in the micrograph.

The density of foam and unfoamed samples was determined from the sample weight in air and water respectively, according to ASTM D 792 method A. The density of the foamed sample is divided by the density of the unfoamed sample to obtain the relative density (ρ_r). The volume fraction occupied by the microvoids (V_f) was calculated as

$$V_f = 1 - \frac{\rho_f}{\rho_m} \quad (5)$$

where ρ_m and ρ_f are the density of the unfoamed polymer and foamed polymer respectively.

The cell density (N_0) based on the unfoamed sample was calculated as

$$N_f = \frac{V_f}{\frac{\pi}{6} D^3} \quad (6)$$

$$N_0 = \frac{N_f}{1 - V_f} \quad (7)$$

where V_f is the volume fraction occupied by the microvoids, N_f is the cell density based on the foamed sample.

Experimental design

In the statistical experimental design, cell size, cell density and relative density of polypropylene/waste ground rubber tire powder (PP/WGRT) foams produced using supercritical carbon dioxide (scCO₂) as a physical blowing agent were studied. The factors consist of WGRT content, saturation pressure of CO₂ and saturation temperature each at three levels. The experiments were performed based on a central composite design. The levels of coded factor are defined as:

$$\text{coded factor levels} = \frac{\text{Actual value} - \text{Factor mean}}{(\text{Range of the factorial value} / 2)}$$

The coded levels appear as -1, 0, and +1 in the design matrix, i. e. -1 for low levels, +1 for high levels, and 0 for centerpoint.

The experimental data presented in Table 1 were analyzed using Rubber Computer Aided Design (hereafter called RCAD, developed by Qingdao University of Science and Technology, China) software in order to determine the key components that had significant effects on the foam structure. Table 1 represents the design for three factors at three levels each. In the design five replicates were used to estimate the experimental error. A regression model relating the response y to P (saturation pressure), T (saturation temperature) and f (WGRT content) that is supported by the design is

$$y = \beta_0 + \beta_1 P + \beta_2 T + \beta_3 f + \beta_{12} PT + \beta_{13} Pf + \beta_{23} Tf + \beta_{11} P^2 + \beta_{22} T^2 + \beta_{33} f^2 + \varepsilon \quad (8)$$

Note that Table 1 was ordered according to the processing conditions, the testing order were randomized.

Acknowledgements

The authors acknowledge the support from the BK21 program in South Korea.

References

- [1] Suh, K. W.; Park, C. P.; Maurer, M. J.; Tusim, M. H.; Genova, R. D.; Broos, R.; Daniel, P. S. *Adv. Mater.* **2000**, 12, 1779.
- [2] Krause, B.; Sijbesma, H. J. P.; Münüklü, P.; Van der Vegt, N. F. A.; Wessling, M. *Macromolecules* **2001**, 34, 8792.
- [3] Doroudiani, S.; Park, C.B.; Kortschot, M.T. *Polym. Eng. Sci.* **1999**, 36, 2645.
- [4] Collias, D. I.; Baird, D. G.; Borggreve, R. J. M. *Polymer* **1994**, 35, 3978.
- [5] Goel, S. K.; Beckman, E. J. *Polym Eng Sci* **1994**, 34, 1137.